Collisional decomposition of the sulfur hexaflouride anion (SF_6^-)

R. L. Champion, I. V. Dyakov, and B. L. Peko[a)]
Department of Physics, College of William and Mary, Williamsburg, Virginia 23187

Yicheng Wang
National Institute of Standards and Technology, Gaithersburg, Maryland 20899-8113

(Received 20 March 2001; accepted 3 May 2001)

Insulating gas mixtures containing SF_6 have been promoted to serve as replacements for pure SF_6 in order to reduce SF_6 atmospheric emission. It has been argued that some synergism may be achieved by choosing proper buffer gases in mixtures with SF_6 such that the buffer gases efficiently slow down electrons into an energy range where the electron attachment cross section for SF_6 is large. A complete understanding of the dielectric properties of SF_6 mixtures obviously requires information about electron detachment from SF_6^- as collisional electron detachment may be the principal source of discharge initiation in SF_6 mixtures. In this paper, we report total cross-section measurements for electron detachment and collision induced dissociation for collisions of SF_6^- with N_2 for collision energies ranging up to a few hundred eV. The experimental results are analyzed using a two-step collision model where the unimolecular decomposition of collisionally excited SF_6^- ions is described in a statistical framework. © *2001 American Institute of Physics.*
[DOI: 10.1063/1.1380692]

I. INTRODUCTION

Sulfur hexafluoride (SF_6) is widely used as a gaseous dielectric in high-voltage applications due to its extremely large cross section for electron attachment[1–3] and stability of SF_6^- with respect to decomposition in subsequent collisions with SF_6.[4] It is also recognized as a potent greenhouse gas and it has been suggested that a mixture of SF_6 and N_2 might serve as a substitute for pure SF_6 in certain applications which require gaseous dielectrics.[5,6] Even with a very low SF_6 content, a SF_6/N_2 mixture exhibits many of the desirable properties of SF_6 as a gaseous dielectric. It has been suggested that this mixture may constitute a synergistic combination: The buffer gas (N_2) serves to cool energetic electrons into the low-energy region where the electronegative gas (SF_6) captures them with a remarkably high cross-section, thereby inhibiting the buildup of free electrons that could cause ionization leading to electrical breakdown. The dielectric properties of this mixture have been the subject of numerous recent investigations.[5,6]

Collisions of SF_6^- with N_2, which result in the decomposition of SF_6^-, are obviously involved in such mixtures when used as gaseous insulators. Cross sections for electron attachment to SF_6 along with those associated with the decomposition of SF_6^- can partially characterize the arc-quenching properties of the mixture, viz., the ability of the mixture to capture free electrons and keep them bound in subsequent collisions. The collisional decomposition of SF_6^- will also be an important reaction pathway leading to creation of chemical by-products and thus needs to be understood in order to fully characterize the dielectric and chemical stability of SF_6/N_2 mixtures. The purpose of this paper is to report the measurement of total cross sections, σ_i $(i=1,2,3)$, for the following three least endothermic reactions:

$$\begin{aligned} SF_6^- + N_2 &\rightarrow SF_6 + e^- + N_2 ; Q_1 = -1.06\ \text{eV} \\ &\rightarrow SF_5^- + F + N_2 ; Q_2 = -1.18\ \text{eV} \\ &\rightarrow SF_5 + F^- + N_2 ; Q_3 = -1.58\ \text{eV}, \end{aligned} \tag{1}$$

for the laboratory collision energies, E_{lab}, ranging from 17 eV to 417 eV. The threshold energies given in Eq. (1) for each channel, Q_i, are for ground state reactants and products.[7,8]

II. EXPERIMENTAL METHOD

The experimental apparatus and techniques used to measure total cross sections for collisional electron detachment and collision induced dissociation (CID) of SF_6^- have been described in detail elsewhere,[4] and only the pertinent details will be given here. The ion source producing SF_6^- used a mixture of 7% SF_6 and 93% Ar at a pressure of about 2 Pa. Thermionically emitted electrons attach to SF_6 and energy analysis of the resulting SF_6^- beam shows that SF_6^- ions form near the filament where the electron energy is low and electron attachment cross sections are high. The negative ions are extracted from the source, mass analyzed and focused into a cylindrically symmetric electrostatic trapping cell, where the molecular anion collides with N_2 at a pressure of $\sim 5 \times 10^{-2}$ Pa. Retardation grids are used to ascertain the energy of the primary ion beam and to separate the collision products according to their energy. A longitudinal magnetic field of about 10 G is used to isolate and confine detached electrons which are collected on a small plate parallel to the grids. A typical retardation analysis of CID ions for collisions of SF_6^- with N_2 at $E_{\text{lab}}=120$ eV is shown in Fig. 1. The

[a)]Present address: Dept. of Physics, University of Denver, 2112 E. Wesley Ave., Denver, Colorado 80208.

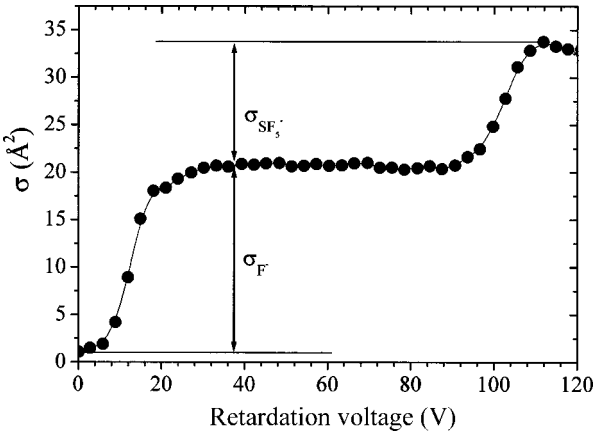

FIG. 1. Retardation analysis of product ions for collisions of SF_6^- with N_2 at $E_{lab}=120$ eV. The slight decrease for V>110 volts is unavoidable due to subtracting "gas in" from "gas out" signals, as the former contain some nonreactive inelastic scattering.

diagram supports the assumption that product ions approximately retain the primary ion's laboratory velocity in the dissociation process as described in Ref. 4. In Fig. 1 each subsequent plateau corresponds to the CID ions with higher energy. The first plateau represents complete retardation of F^-, while the second plateau is due to SF_5^-. At lower collision energies ($\lesssim$11 eV in the center of mass frame), difficulties in determining the cross section for SF_5^- production result from large angle elastic and inelastic scattering of the primary ion beam. The cross sections for σ_1, σ_2, and σ_3 are thought to be accurate to within 10%, 25%, and 15%, respectively. The large uncertainty for σ_2 is due to this large angle elastic/inelastic scattering of SF_6^-.

III. RESULTS AND DISCUSSION

The measured cross sections for electron detachment and CID of SF_6^- by N_2 are presented in Fig. 2 as a function of relative collision energy, E_{rel}. It is interesting to observe that although electron detachment has the lowest threshold energy for decomposition, CID is the dominant decomposition mechanism for the anion, except for the lowest collision energies. The CID channel leading to the production of F^- has a higher energetic threshold than that for SF_5^-, which may be attributed to the higher electron affinity of SF_5. The electron detachment cross section exhibits a minimum for $E_{rel}\sim 25$ eV and increases sharply thereafter. These features are strikingly similar to previous observations for collisions of SF_6^- with rare gases,[4] as can be seen in Fig. 3, where the electron detachment cross sections for $SF_6^-+N_2$ are shown along with previous results for the targets He, Ne and Ar. Such target-independent results are often described by a two-step mechanism where collisional excitation of SF_6^- by the target X is followed by its unimolecular decomposition; viz.,

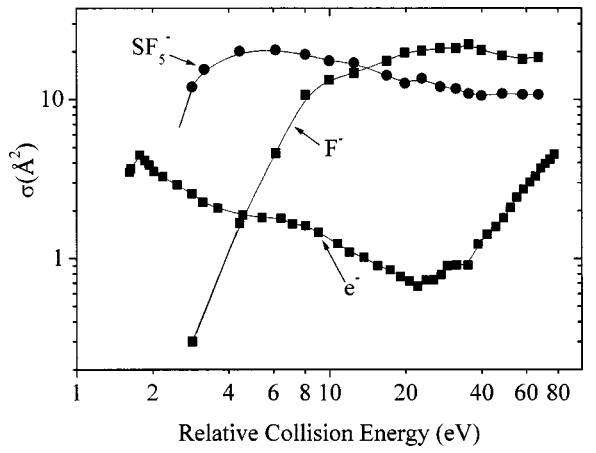

FIG. 2. The cross sections for electron detachment and CID of SF_6^- by N_2 as a function of E_{rel}.

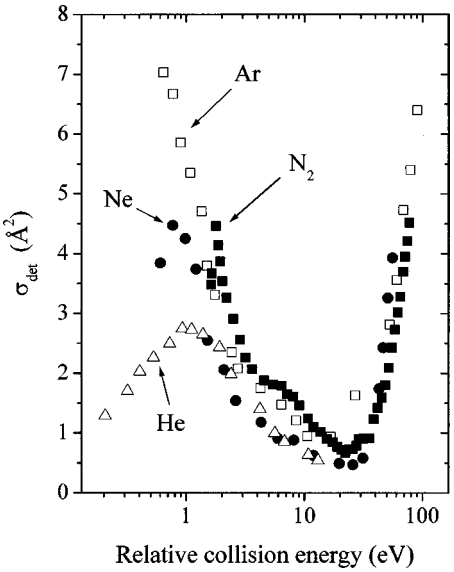

FIG. 3. Comparison of the electron detachment cross sections for collisions of SF_6^- with N_2, He, Ne, and Ar.

$$SF_6^- + X \rightarrow SF_6^{-*}(U, J_0) + X \swarrow e^- \text{ or } F^- \text{ or } SF_5^-, \quad (2)$$

where U is the total internal energy of the unstable, excited SF_6^{-*} product which is partitioned rovibrationally and J_0 is the rotational quantum number, indicating that portion of U which is rotational energy.

The overall dominance of CID over electron detachment for collision energies, where all the reaction channels are energetically accessible, can be qualitatively understood with the help of the unimolecular decomposition model originally proposed by Klots.[9,10] In this model, the decomposition rates of SF_6^{-*} for products given in Eq. (1) may be expressed by

$$k_i(U,J_0) = \frac{\beta_i}{h(2J_0+1)\rho_{vib}^{(SF_6^-)^*}(E_{vib})} \times \int_{\varepsilon=0}^{U_i=U-Q_i} \rho_{vib}^{product}(\varepsilon) \sum_J \sum_L (2J+1)\, d\varepsilon, \quad (3)$$

assuming that $(SF_6^-)^*$ and polyatomic products of its decomposition can be treated as spherical tops. In the expression

above ρ_{vib} is the vibrational density of states, J is the rotational angular momentum of the product spherical top, L is the orbital angular momentum of the products, β_i is the ratio of the symmetry numbers of $(SF_6^-)^*$ and the product spherical top. The vibrational density of states can be approximated[11] as

$$\rho_{vib}(\varepsilon)=\frac{(\varepsilon+\varepsilon_0)^{s-1}}{(s-1)!\prod_{i=1}^{s} h\nu_i}, \tag{4}$$

where ε_0 is the zero-point energy, ε is the energy above the zero-point level, s is the number of vibrational degrees of freedom, and ν_i are the vibrational frequencies. It is not necessary to consider excited electronic states of the anion in this treatment as, for a given U, the vibrational density of states of any excited electronic state will be negligible compared to that for the ground state.

To evaluate Eq. (4), the values of vibrational frequencies ν_i for SF_6^-, SF_6, SF_5^-, and SF_5 were taken from recent calculations by Lugez *et al.*[12] Not all of these vibrational frequencies are known experimentally. Where both the calculated and experimentally determined frequencies exist (SF_6, for example), their differences are in the range of 10%. It is important to point out that a change of this magnitude for ν_i does not alter the conclusions which arise from these calculations in any substantive manner.

The internal energy, U, of $(SF_6^-)^*$ was assumed to partition equally among its three rotational and fifteen vibrational degrees of freedom. The initial angular momentum quantum number, J_0, was then calculated according to

$$E_{rot}=BJ(J+1) \tag{5}$$

for a spherical top where B is the rotational constant. The threshold energies, Q_i, for electron detachment and CID into SF_5^- or F^- given in Eq. (1) were used in the calculation. There exist some uncertainties about these threshold energies, but there is a general agreement on the order in which these values follow.[7,8]

The restrictions on the product angular momentum quantum numbers J and L in Eq. (3) were determined as follows: For electron detachment, s-electrons dominate the detachment mechanism or $L=0$ and $J=J_0$. For CID channels 2 and 3, once a value of ε is chosen, the rotational energy, E_{rot} of the product spherical top can range from zero to U-Q_i-ε. The range of J is then calculated according to Eq. (5). Two factors determine the range of L in Eq. (3): The triangle rule $|J-J_0|\leqslant L\leqslant J+J_0$ and the Langevin orbiting restriction[9]

$$L_{max}(L_{max}+1)=\gamma(U-Q_i-\varepsilon-E_{rot}).$$

Here,

$$\gamma=2^{3/2}\mu e\alpha^{1/2}/\hbar^2,$$

where μ is the reduced mass of the CID products, and α is the polarizability of the neutral product. In these calculations we assumed that SF_5^-, when its internal energy is high enough, would itself decompose. The decomposition channel for SF_5^-, which has the lowest threshold energy, is F^-+SF_4 (1.1 eV).[12] The threshold energies for decomposing into SF_4^-+F (3.0 eV) and e^-+SF_5 (3.8 eV)[12] are significantly higher, and, as will become clear later in this paper, they are beyond the energy range of the present treatment. The decomposition rate, k_4, for $SF_5^-\rightarrow F^-+SF_4$ was calculated using the same statistical model, with vibrational frequencies also taken from the work of Lugez *et al.*[12] The decomposition of SF_5^- produces a source for F^- and a sink for SF_5^-. The production rate of F^- via SF_5^- is governed by the rate of the slower, rate-determining step of the overall reaction, with a characteristic time $\tau=1/k_2+1/k_4$. The combined effective rate for F^- production from $(SF_6^-)^*$ is then $k_3^{eff}=k_3+1/\tau$, and for SF_5^- production, it is $k_2^{eff}=k_2-1/\tau$. Of course, $k_1^{eff}=k_1$, as we have considered no additional source or sink of electrons.

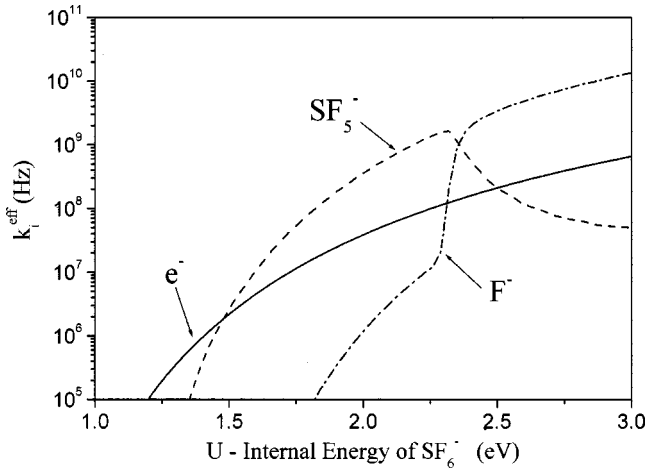

FIG. 4. Calculated decomposition rates, k_1, k_2^{eff}, and k_3^{eff}, are plotted as a function of the internal energy, U, of $(SF_6^-)^*$.

The resulting decomposition rates for $(SF_6^-)^*$ are presented in Fig. 4. The main features which can be immediately observed are as follows. The decomposition rates for the three channels of reaction [Eq. (1)] onset in the order of their internal threshold energies. However, the rates for the CID channels initially rise more steeply with increasing internal energy of SF_6^- than the detachment rate, which can be attributed to the larger phase space for the angular momenta of the CID products than that for the detachment products. The production of SF_5^- becomes the dominant decay mechanism as U increases above 1.5 eV until it reaches around 2.3 eV, where the secondary decomposition rate of SF_5^- rises so steeply that F^- quickly becomes the dominant product ion.

To facilitate comparison between the decomposition rates of $(SF_6^-)^*$ and the decomposition cross sections in collisions of SF_6^- with N_2, we present the calculated branching ratios $k_i^{eff}/(\Sigma k_i^{eff})$ as a function of U in Fig. 5(a) along with the measured branching ratios $\sigma_i/\Sigma(\sigma_i)$ as a function of the relative collision energy, E_{rel}, in Fig. 5(b). As can be seen in the figure, the overall features of the calculated branching ratios resemble the experimentally determined branching ratios; both show that there are three distinct energy regions with different dominant product ions. This comparison clearly shows that the model calculation can be used to better understand the experimental results. As the collision energy increases, more translational energy is converted into the internal rovibrational excitation energy of $(SF_6^-)^*$. The first

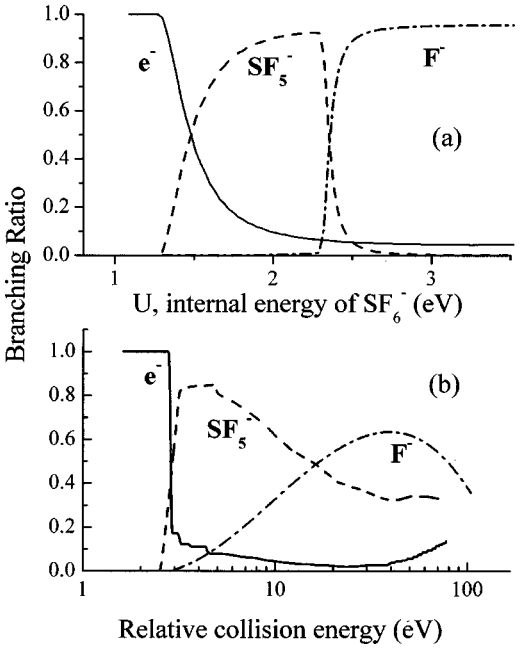

FIG. 5. (a) Calculated branching ratios $k_i^{\mathrm{eff}}/(\Sigma k_i^{\mathrm{eff}})$ as a function of U; (b) measured branching ratios $\sigma_i/\Sigma(\sigma_i)$ as a function of E_{rel}.

energetically allowed decomposition channel for $(SF_6^-)^*$ is the electron detachment. The detachment probability quickly decreases, however, as the collision energy increases because the rate for the competing CID channel leading to $SF_5^- + F$ rises faster. As U is increased further, SF_5^- becomes the dominant product ion in the intermediate energy region. The calculation also reveals that the decomposition rate for $SF_5^- \rightarrow F + SF_4$ rises steeply as the internal energy increases above its decomposition threshold and this secondary process may, in fact, be the main source of F^- ions detected in collisions of SF_6^- with N_2. The statistical model cannot, however, explain why the detachment cross section, $\sigma_1(E_{\mathrm{rel}})$, rises for $E_{\mathrm{rel}} \geqslant 30$ eV. This increase observed for $\sigma_1(E_{\mathrm{rel}})$ is undoubtedly due to a competing, direct detachment mechanism which is distinct from that which follows collisional excitation of SF_6^-.

The results of Fig. 5 suggest that, to a rough approximation, a mapping of $U(E_{\mathrm{rel}})$ might be given by $U(E_{\mathrm{rel}}) \approx [1 + \log_{10}(E_{\mathrm{rel}}/\mathrm{eV})]$ eV. It is clear from Fig. 4 that any primary SF_6^- ions formed by attaching electrons with energies less than 0.2 eV will, although metastable, clearly survive their trip from the source to the collision region, a transit requiring about 10 μsec. Hence the mean internal energy, U^0, of the SF_6^- ion *prior* to its collision with N_2 is fairly well-defined and will be slightly in excess of the electron affinity of SF_6. The collision then provides the additional excitation, $U^{\mathrm{add}} \approx [\log_{10}(E_{\mathrm{rel}}/\mathrm{eV})]$ eV, with $U = U^0 + U^{\mathrm{add}}$. Obviously there is no simple, unique correspondence between E_{rel} and U; the mapping is clearly much more complicated than given above. Nevertheless, it is interesting to note that one can characterize certain aspects of an extremely complicated inelastic collision with such a simple model.

IV. SUMMARY

Absolute total cross sections for electron detachment and collision-induced dissociation have been measured for collisions of SF_6^- with N_2 for laboratory collision energies from 17 eV to 417 eV. Electron detachment cross sections are below 4.5 Å^2 with minimum of $\sim$1 Å^2 at $E \sim 20$ eV. These cross sections are higher than those for the SF_6 target[4] and can partly account for lower dielectric properties of a SF_6/N_2 mixture compared to those of pure SF_6. Collision induced dissociation processes provide the dominant destruction mechanism for SF_6^- with absolute cross sections approaching 35 Å^2 at higher energies. The decomposition cross sections of SF_6^- in collisions with N_2 are similar to those observed for rare gas targets. The target-independent features of SF_6^- decomposition can be qualitatively explained using a two-step model in which collisional decomposition is followed by unimolecular decomposition. This model shows that the dominance of CID processes result from the larger phase space for the CID channels than the electron detachment. The model calculation also suggests that the main source of F^- ions detected in collisions of SF_6^- with N_2 may result from subsequent decomposition of excited SF_5^-.

ACKNOWLEDGMENT

This work was supported in part by the U.S. Department of Energy, Office of Energy Science, Division of Chemical Sciences.

[1] L. G. Christophorou and J. K. Olthoff, J. Phys. Chem. Ref. Data **29**, 267 (2000).
[2] L. E. Kline, D. K. Davies, C. L. Chen, and P. J. Chantry, J. Appl. Phys. **50**, 6789 (1979).
[3] A. Chutjian and S. H. Alajajian, Phys. Rev. A **31**, 2885 (1985).
[4] Y. Wang, R. L. Champion, L. D. Doverspike, J. K. Olthoff, and R. J. Van Brunt, J. Chem. Phys. **91**, 2254 (1989).
[5] L. G. Christophorou and R. J. Van Brunt, IEEE Trans. Dielectr. Electr. Insul. **2**, 952 (1995).
[6] L. G. Christophorou, J. K. Olthoff, and D. S. Green, "Gases for Electrical Insulation and Arc Interruption: Possible Present and Future Alternatives to Pure SF_6," NIST Tech. Note **1425**, 1 (1997).
[7] D. Smith, P. Spanel, S. Matejcik, A. Stamatovic, T. D. Mark, T. Jaffke, and E. Illenberger, Chem. Phys. Lett. **240**, 481 (1995).
[8] J. P. Astruc, R. Barbe, A. Lagreze, and J. P. Schermann, Chem. Phys. **75**, 405 (1983).
[9] C. E. Klots, J. Phys. Chem. **75**, 1526 (1971); J. Chem. Phys. **64**, 4269 (1976).
[10] S. E. Haywood, L. D. Doverspike, R. L. Champion, E. Herbst, B. K. Annis, and S. Datz, J. Chem. Phys. **74**, 2845 (1980).
[11] G. Z. Whitten and B. S. Rabinowitch, J. Chem. Phys. **41**, 1883 (1964).
[12] C. L. Lugez, M. E. Jacox, R. A. King, and H. F. Schaefer III, J. Chem. Phys. **108**, 9639 (1998).